Published in final edited form as:
Cancer Res. 2011 November 1; 71(21): 6764–6772. doi:10.1158/0008-5472.CAN-11-0691.

Itraconazole inhibits angiogenesis and tumor growth in non-small cell lung cancer

Blake T. Aftab, **Irina Dobromilskaya**, **Jun O. Liu**, and **Charles M. Rudin**
Sidney Kimmel Comprehensive Cancer Center, Johns Hopkins University, Baltimore MD

Abstract

The anti-angiogenic agent bevacizumab has been approved for the treatment of non-small cell lung cancer, although the survival benefit associated with this agent is marginal, and toxicities and cost are substantial. A recent screen for selective inhibitors of endothelial cell proliferation identified the oral anti-fungal drug itraconazole as a novel agent with potential anti-angiogenic activity. Here we define and characterize the anti-angiogenic and anti-cancer activities of itraconazole in relevant preclinical models of angiogenesis and lung cancer. Itraconazole consistently demonstrated potent, specific, and dose-dependent inhibition of endothelial cell proliferation, migration, and tube formation in response to both vascular endothelial growth factor (VEGF)- and basic fibroblast growth factor (bFGF)-mediated angiogenic stimulation. In vivo, using primary xenograft models of human non-small cell lung cancer, oral itraconazole showed single agent growth-inhibitory activity associated with induction of tumor HIF1α expression and marked inhibition of tumor vascularity. Itraconazole significantly enhanced the anti-tumor efficacy of the chemotherapeutic agent cisplatin in the same model systems. Taken together, these data suggest that itraconazole has potent and selective inhibitory activity against multiple key aspects of tumor-associated angiogenesis in vitro and in vivo, and strongly support clinical translation of its use. Based on these observations we have initiated a randomized phase II study comparing the efficacy of standard cytotoxic therapy with or without daily oral itraconazole in patients with recurrent metastatic non-small cell lung cancer.

INTRODUCTION

Angiogenesis, the summation of multiple cellular and biological processes culminating in the propagation of blood vessels, has been the subject of extensive examination in the context of tumor biology over the past four decades since first proposed by Judah Folkman in 1971 (1). Solid tumor growth and progression is dependent on tumor-associated angiogenesis. Tumor expression and circulating levels of angiogenic factors have been correlated with aggressive tumor growth, predilection for metastasis, and prognosis in a wide array of solid tumors, including lung cancer (2–4). Although many putative regulators of angiogenesis have been identified, two secreted factors, vascular endothelial growth factor (VEGF) and basic fibroblast growth factor (bFGF) have been particularly strongly implicated in tumor-associated angiogenesis (5). VEGF and bFGF interact with distinct families of tyrosine kinase receptors (RTK) on the surface of endothelial cells, and activate multiple downstream signaling pathways. Together these pathways promote endothelial cell

Corresponding author: Charles M. Rudin, MD, PhD, Professor of Oncology, The Sidney Kimmel Comprehensive Cancer Center at Johns Hopkins, Cancer Research Building 2, Room 544, 1550 Orleans Street, Baltimore, MD 21231, **Tel:** 410-502-0678, **Fax:** 410-502-0677, rudin@jhmi.edu.

Relevant financial disclosures: The intellectual property covering itraconazole has been licensed from Johns Hopkins University to Accelas Holdings, Inc. in which J.O.L. owns equity.

survival, proliferation, migration, invasion, and tube formation, resulting in formation of new vascular networks (6; 7).

Lung cancer is the leading cause of cancer mortality in both men and women in the US (8). The only anti-angiogenic therapy currently approved for use in lung cancer is the α-VEGF monoclonal antibody bevacizumab. A landmark phase III clinical study, ECOG 4599, randomized patients with advanced non-small cell lung cancer (NSCLC) to a standard chemotherapy doublet with or without bevacizumab (9). This study demonstrated a statistically significant improvement in both progression-free and overall survival in favor of the bevacizumab-containing arm. There are, however, major limitations to the clinical utility of bevacizumab. The absolute improvements in progression-free and overall survival in this study were modest (1.7 and 2 months, respectively). Due to episodes of fatal hemoptysis in a prior study (10), enrollment was restricted to patients with non-squamous tumors, with no history of hemoptysis, with no brain metastases, with no indication for use of anti-coagulants, and with good performance status. Even in this carefully selected subpopulation bevacizumab use was associated with increased treatment-related deaths ($p = 0.001$) including 5 episodes of fatal hemoptysis (vs. 0 on the control arm), and with significantly increased rates of hypertension, proteinuria, bleeding, neutropenia, febrile neutropenia, thrombocytopenia, hyponatremia, rash, and headache ($p < 0.05$ for each of these). Across disease types, bevacizumab use has been associated with increased treatment-related mortality (11). The financial cost of bevacizumab, given the limited efficacy and significant toxicity, was seen by many as excessive, at upwards of $500,000 per year of life gained (12; 13). A final concern comes from what was intended as a “confirmatory” trial, the AVAiL study, which randomized a similar patient population to a different standard chemotherapy doublet with or without bevacizumab (14). This study failed to demonstrate a statistically significant difference in survival. In summary, while evidence is strong that angiogenesis is critical to tumor growth and progression, less toxic, less cost-prohibitive, and more effective therapies are needed. These observations strongly support further development of novel anti-angiogenic strategies for patients with lung cancer.

Itraconazole is an orally bioavailable, FDA-approved agent belonging to the family of azole antifungal drugs, which inhibit the enzyme lanosterol 14α-demethylase (14-DM) responsible for the conversions of lanosterol to ergosterol in fungi and lanosterol to cholesterol in humans, respectively. Initially reported by Chong *et al.*, itraconazole has been identified as a potent inhibitor of endothelial cell proliferation and matrigel stimulated angiogenesis, with inhibition of 14-DM and sterol biosynthesis only partially explaining this novel anti-proliferative activity (15). Further efforts to characterize the mechanism of inhibition of endothelial cell proliferation are ongoing, with recent reports suggesting perturbation of cholesterol trafficking pathways imparted by itraconazole as a possible mechanism contributing to this activity (16). Of note, itraconazole has also recently been implicated as an antagonist of the hedgehog signaling pathway in models of hedgehog pathway deregulation (17). Pre-clinical evaluation of the anti-angiogenic capacity of itraconazole in relevant *in vitro* models of angiogenesis and *in vivo* models of cancer are clearly required in order to determine the viability of pursuing further clinical development of itraconazole as an anti-angiogenic agent.

Tumor cell lines implanted into immunodeficient mice comprise the most commonly used platform for *in vivo* preclinical cancer therapeutic testing. However, *ex vivo* derivation of stable cell lines in tissue culture is associated with profound changes in cellular morphology, growth characteristics, chromosome structure, gene copy number, and gene expression (18–20), changes which are not reversed by reintroduction of cell lines into mice (21). In sharp contrast to the harsh biological conditions in which tumors naturally arise, typical tissue culture conditions include relatively high oxygen tension, high glucose concentration, and

low hydrostatic and oncotic pressures. These are precisely conditions in which maintenance of angiogenic drive, in particular, is not relevant. To evaluate the *in vivo* effects of itraconazole, here we employ an alternative approach based on primary lung cancer xenografts. The primary xenograft model depends on immediate transfer of human cancers from patients into recipient mice, without intervening tissue culture or cell line derivation *ex vivo*. We have previously reported that gene expression profiles of lung cancer primary xenografts more closely reflects those of the human cancers than do profiles of cell lines derived from the same parental tumor when re-implanted as standard (secondary) xenografts (21). These observations are supported by data from other investigators exploring primary xenografts (22; 23).

Here we describe the results of a series of *in vitro* and *in vivo* analyses evaluating the putative anti-angiogenic activities of itraconazole. We employ several *in vitro* assays using human umbilical vein endothelial cells (HUVEC) to separately probe specific hallmarks of endothelial cell function as they relate to angiogenic processes. These functional competencies include proliferative capacity, migration, chemotactic potential, and the ability to spontaneously form an extracellular matrix (ECM) supported tube network. The capacity of itraconazole to modulate these functions was explored in the presence of multiple angiogenic stimuli including VEGF and bFGF. We further investigate the *in vivo* activity of itraconazole as an inhibitor of tumor-associated angiogenesis and of tumor growth, both as a single agent and in combination with standard cytotoxic chemotherapy. These studies offer the first assessment of the efficacy of itraconazole as an anti-angiogenic agent and as an anti-cancer therapeutic in a primary disease model.

MATERIALS AND METHODS

Cell Culture and Reagents

HUVEC (Lonza) were grown in endothelial cell growth medium-2 (EGM-2, Lonza) per manufacturer's recommendations. Cells were washed with phosphate-buffered saline (PBS) and serum-starved in endothelial cell basal medium-2 (basal media, Lonza) supplemented with 0.5% bovine serum albumin (BSA, Sigma) for 4–6 h prior to assays. NSCLC cell lines, NCI-H358, NCI-H1838, NCI-H596 and NCI-H1975 were obtained from ATCC and cultured in RPMI-1640 supplemented with 10% fetal bovine serum (FBS) per ATCC recommendations. Cultures from LX-7 and LX-14 tumors were derived from preparations of single-cell suspensions grown in Media-2 plus 4.5 g/L glucose (RPMI-1640 supplemented with 10% FBS, 2 mM L-glutamine, 1 mM sodium pyruvate, 10 mM HEPES buffer, and 1.5 g/L sodium bicarbonate). Cultures were incubated at 37°C with 95% air / 5% CO_2 in a humidified incubator, unless otherwise stated. Itraconazole was obtained from Sigma and prepared as a solution in dimethyl sulfoxide (DMSO) for use in i*n vitro* experiments. Itraconazole oral solution (Sporanox, Ortho Biotech) and cisplatin (APP Pharmaceuticals) for *in* vivo experiments were obtained from the pharmacy of The Sidney Kimmel Comprehensive Cancer Center and diluted as necessary with 40% hydroxypropylcyclodextrin, 2.5% propylene glycol, pH 4.5 in water and saline, respectively.

Proliferation Assays

HUVEC were suspended in either EGM-2 or basal media containing 0.5% BSA and supplemented with 10 ng/ml VEGF-A or 12 ng/ml bFGF. NCI-H358, NCI-H1838, NCI-H596, NCI-H1975, LX-7, and LX-14 cells were suspended in respective RPMI-1640 based media. Cells were seeded at $1 – 5 \times 10^3$ cells per well and allowed to attached for a period of 6 h. Cells were then exposed to vehicle or drug treatment and incubated for 48 h. Duplicate plates containing NCI-H358, NCI-H1838, and NCI-H596 cells were also cultured under hypoxic conditions generated by flushing a modular incubator chamber with a 95% N_2/5%

CO_2 pre-analyzed air supply to generate a stable atmosphere of 1.5% O_2. Relative cell numbers following incubation were quantified by CellTiter 96® AQ_{ueous} One Solution Cell Proliferation Assay (Promega) per manufacturer's recommendations using a SpectraMax $M2^e$ spectrophotometer and SoftMax Pro software (Molecular Devices).

Phospho-RTK Analysis

HUVEC were cultured on 10 cm culture treated dishes in EGM-2 medium and treated with vehicle or itraconazole for 24 h. Cells were then harvested using a cell scraper and pelleted by centrifugation (300×g). Cells were then resuspended and lysed in modified RIPA buffer [150 mM NaCl, 50 mM Tris (pH 7.4), 1% NP-40, 0.25% Na-deoxycholate, 1 mM EDTA, 1 mM PMSF, 1 mM Na-orthovanadate, 1 mM NaF, 1× Phosphatase Inhibitor Cocktails 1 and 2 (P2850 and P5726, respectively, Sigma), and 1× Protease Inhibitor Cocktail (P8340, Sigma)], followed by centrifugation, yielding clarified lysates. Total protein content was quantified using Bradford assay. Lysates were analyzed using Proteome Profiler™ Human Phospho-RTK Array (R&D Systems) per manufacturer's recommendations using 100 μg total protein.

Migration Assays

Transwell Cell Migration Assay—EGM-2, or basal media containing 0.5% BSA supplemented with 10 ng/ml VEGF-A or 12 ng/ml bFGF was added to the lower wells of a CytoSelect Fluorometric 8 μM Transwell Migration Assay plate (Cell Biolabs). Cells were suspended in basal media supplemented with 0.5% BSA and added to the upper wells of the plate and exposed to vehicle or drug treatment followed by incubation for 16 h to allow for migration across the porous membrane. Cells remaining in the upper wells were then voided. Migratory cells were detached from the lower face of the transwell membrane and lysed. Total DNA in the resulting lysates was stained using CyQuant GR dye (Millipore) and quantified by fluorometric analysis per manufacturer's recommendations.

Oris Cell Migration Assay—HUVEC were plated at 95% confluency in Oris Cell Migration Assay plates (Platypus Technologies) and incubated overnight to allow cell attachment. Wells were rinsed with PBS and incubated in basal media for 6 h. Stopper inserts were then removed to reveal a migration zone of 2 mm diameter and cells were again rinsed in PBS followed by exposure to EGM-2 media containing itraconazole (0–3 μM), or basal media supplemented with 0.5% BSA. Assay plates were incubated for 24 h to permit cell migration. Following migration, cells were labeled with 2 μg/ml calcein-AM for 30 min and visualized using an Olympus BX61 fluorescence microscope with images captured using an affixed CCD camera and Slidebook™ 5 software (Intelligent Imaging Innovations). Migration was quantified using ImageJ software (NIH) to measure the area of the migration zone remaining post migration and reported as the percent decrease in migration zone area from start of the migration period.

Tube Formation Assay

Wells of an assay plate were coated with growth factor reduced basal membrane extract (Geltrex, Invitrogen) and were incubated for 30 min at 37°C. HUVEC were then suspended in either EGM-2 or basal media containing 0.5% BSA supplemented with 12 ng/ml VEGF or 10 ng/ml bFGF and seeded at 1.5×10^4 cells per well. Cells were exposed to treatment followed by 16 h incubation. Cells and resulting tube networks were visualized following 30 min incubation with 2 μg/ml Calcein AM using an Olympus BX61 fluorescence microscope.

NSCLC Primary Xenograft Models

The primary NSCLC xenograft models LX-14 and LX-7, representing squamous cell and adenocarcinoma histologies, respectively, were derived from primary tumor tissue obtained from treatment-naïve patients at the Sidney Kimmel Comprehensive Cancer Center.. In brief, tumor cells isolated from bronchoscopic biopsy specimens were prepared into single-cell suspensions, mixed with Matrigel in equal volume, and injected as a subcutaneous (s.c.) bolus into NOD/SCID mice. Primary xenograft tumors were maintained solely in immunocompromised mice by serial passaging. Tumor sections of primary xenografts were formalin fixed, sectioned, and stained with hematoxylin and eosin at various passages to verify that they consistently maintained NSCLC histology characteristics. Tissues were characterized for KRAS and EGFR mutations, EML4-ALK translocation, and cMET amplification by the Molecular Pathology Laboratory at Johns Hopkins University (Table S1, supplemental data on line).

Freshly isolated primary xenograft tumors were mechanically dissociated into single-cell suspensions; 2.5×10^6 viable cells were suspended in equal volumes of PBS and Matrigel and implanted s.c. in adult homozygous NOD/SCID mice (Charles River Laboratories). Once tumors reached ≥150 mm^3, calculated as $V = L \times W^2 / 2$, mice were treated with either vehicle control, itraconazole [75 mg/kg oral twice daily (bid)], cisplatin [4 mg/kg intraperitoneal (i.p.) q7d], or a combination of itraconazole and cisplatin. All treatments were administered in 10 ml/kg volumes with 12 h separation between bi-daily treatments.

Statistical analyses were performed for each primary xenograft separately. Initial tumor volume measurements are summarized using means, standard error of the mean (SEM), and ranges. Growth patterns were summarized graphically by plotting the mean and SEM for each treatment group over time. Treatment groups were analyzed by 2-tailed paired student t-test with $p<0.05$ considered statistically significant.

Immunoblot Analyses

Tumors were harvested 4 h post-last dose following a 14-day treatment in tumor bearing mice. Tumors were mechanically homogenized in 1:11 (w:v) modified RIPA buffer. Clarified lystates were then generated by centrifugation of crude lysates. Total protein content of was quantified by Bradford assay and equally pooled by treatment group. Pooled lysates were mixed with lithium dodecyl sulfate sample buffer (Invitrogen), heated to 70 °C for 5 min, and resolved by electrophoresis on a 4–12% Bis-Tris NuPage gel (Invitrogen). Protein was then electrophoretically transferred to polyvinylidene fluoride membranes. Membranes were blocked using 5% condensed milk in Tris-buffered saline containing 0.2% Tween 20. Primary goat polyclonal antibodies to HIF1α (sc-8711) and β-actin (sc-1615, Santa Cruz Biotechnology) were used at a final dilution of 1:100 and 1:500, respectively. The secondary horseradish peroxidase-linked bovine anti-goat IgG antibody (sc-2352, Santa Cruz Biotechnology) was used at a dilution of 1:1000. Immunodetection was performed using ECL and autoradiographs were scanned using a GS-800 calibrated densitometer and analyzed using Quantity One software (BioRad).

Assessment of Tumor Vascular Area

Nuclei of perivascular cells associated with perfusion competent tumor vessels were detected by *in vivo* perfusion of Hoescht 33342 (HOE), as previously reported (24; 25). Briefly, animals were injected intravenously with 15 mg/kg HOE saline solution in a 10 ml/kg volume 4 h post last dose. Animals were euthanized by cervical dislocation 1.5 min following injection. Tumors were then harvested and frozen in Tissue Tek O.C.T. compound (Sakura Finetek). Tumors were serially sectioned with 6 μm thickness, mounted on Superfrost glass slides (Fisher) and allowed to air dry overnight. Tumor sections were then

scanned and HOE staining of perivascular nuclei visualized under 10× objective on an Olympus BX61 fluorescence microscope affixed with an automated stage using Slidebook 5 software (Intelligent Imaging Innovations) to generate whole section montage images. Tumor images were processed using ImageJ software by applying a threshold across all tumor images to generate binary representations of HOE positive perivascular signal with hole filling used to approximate perfused vessel area (24). Perfused vessel area was then quantified as a percent of total tumor area for each tumor sample and mean vessel area ± SEM is reported as a percent of total tumor area for each treatment group.

RESULTS

Itraconazole inhibits HUVEC proliferation but has no direct anti-proliferative effects on NSCLC cells

We initially sought to confirm the inhibitory activity of itraconazole on endothelial cell proliferation, and to evaluate the specificity of this effect for distinct angiogenic stimuli. Itraconazole demonstrated equipotent, dose-dependent inhibition of HUVEC in all growth factor stimulated conditions tested, including stimulation with VEGF, bFGF, bFGF/VEGF or EGM-2 media (containing these and multiple additional growth factors), with approximate IC_{50} (95% CI) values of 588 nM (553–624 nM), 689 nM (662–717 nM), 691 nM (649–733 nM) and 628 nM (585–672 nM), respectively (Figure 1A); (Dunn's test not significant for differences in these values). Since this effect was observed both with VEGF and bFGF, we examined whether itraconazole exposure altered the activity state of the receptors primarily implicated in VEGF- and bFGF-mediated angiogenesis. Analysis of phospho-tyrosine levels on receptor tyrosine kinases (RTK) in HUVEC cultured in EGM-2 revealed dose dependent decreases specifically in phospho-VEGFR2 and phospho-FGFR3 levels (Figure 1B). None of the other receptor tyrosine kinases present on the array were similarly affected. Together these data demonstrate that itraconazole has inhibitory effects on multiple primary angiogenic pathways.

To assess the relative specificity of the inhibitory activity of itraconazole on endothelial cells, versus possible direct effects on tumor cell growth, the anti-proliferative effects of itraconazole were examined in a panel of NSCLC cell lines representing a variety of genetically and phenotypically distinct lung cancer subtypes. In these NSCLC cell lines, itraconazole had no appreciable effect on proliferation below the maximum tested concentration of 100 μM. To mimic effects under varying oxygen tension, as might be seen in tumor cells *in vivo*, the assays were repeated under hypoxic culture conditions, again revealing no change in proliferation at concentrations below 100 μM itraconazole (Table S1, supplemental data on line).

Itraconazole potently inhibits HUVEC migration and chemotaxis

Endothelial cell migration is an essential process in angiogenesis and is functionally distinct from proliferation (26; 27). Migration is regulated by multiple chemotactic stimuli, resulting in the activation of signaling pathways that mediate cytoskeletal remodeling. We explored the effects of itraconazole on endothelial cell migration across stimulus gradients using a Boyden Chamber assay. HUVEC migration was also assessed in a modified wound-healing assay.

The Boyden chamber assay was employed to assess chemotactic potential of HUVEC across gradients of angiogenic factors. Itraconazole inhibited VEGF-stimulated, bFGF-stimulated, and EGM-2-stimulated HUVEC migration in a dose-dependent manner, with similar potencies to those demonstrated in the endothelial proliferation assays above (Figure 2A).

Itraconazole also markedly inhibited migration of HUVEC under non-gradient stimulation with EGM-2, as assessed in the modified wound-healing assay (Figure 2B and C).

Itraconazole potently inhibits HUVEC tube formation

Beyond simple endothelial cell proliferation and chemotactic migration, neovascularization is dependent on angiogenic stimuli driving formation and organization of tubular networks, i.e. a capillary bed, requiring breakdown and restructuring of extracellular connective tissue. This capacity for formation of invasive and complex capillary networks can be modeled *ex vivo* with the provision of ECM components as a growth substrate, promoting spontaneous formation of a highly cross-linked network of HUVEC-lined tubes (28). We utilized this model to further define dose-dependent effects of itraconazole in response to VEGF, bFGF, and EGM-2 stimuli. In this assay, itraconazole inhibited tube network formation in a dose-dependent manner across all stimulating culture conditions tested and exhibited similar degree of potency for inhibition as demonstrated in HUVEC proliferation and migration assays (Figure 3).

Itraconazole inhibits growth of NSCLC primary xenografts as a single-agent and in combination with cisplatin therapy

The effects of itraconazole on NSCLC tumor growth were examined in the LX-14 and LX-7 primary xenograft models, representing a squamous cell carcinoma and adenocarcinoma, respectively. NOD-SCID mice harboring established progressive tumors treated with 75 mg/kg itraconazole twice-daily demonstrated significant decreases in tumor growth rate in both LX-14 and LX-7 xenografts (Figure 4A and B). Single-agent therapy with itraconazole in LX-14 and LX-7 resulted in 72% and 79% inhibition of tumor growth, respectively, relative to vehicle treated tumors over 14 days of treatment ($p<0.001$). Addition of itraconazole to a 4 mg/kg q7d cisplatin regimen significantly enhanced efficacy in these models when compared to cisplatin alone. Cisplatin monotherapy resulted in 75% and 48% inhibition of tumor growth in LX-14 and LX-7 tumors, respectively, compared to the vehicle treatment group ($p<0.001$), whereas addition of itraconazole to this regimen resulted in a respective 97% and 95% tumor growth inhibition ($p\leq0.001$ compared to either single-agent alone) over the same treatment period. The effect of combination therapy was quite durable: LX-14 tumor growth rate associated with a 24-day treatment period of cisplatin monotherapy was decreased by 79.0% with the addition of itraconazole ($p<0.001$), with near maximal inhibition of tumor growth associated with combination therapy maintained throughout the duration of treatment.

Itraconazole treatment increases tumor HIF1α and decreases tumor vascular area in SCLC xenografts

Markers of hypoxia and vascularity were assessed in LX14 and LX-7 xenograft tissue obtained from treated tumor-bearing mice. Probing of tumor lysates by immunoblot indicated elevated levels of HIF1α protein in tumors from animals treated with itraconazole, whereas tumors from animals receiving cisplatin remained largely unchanged relative to vehicle treatment (Figure 4C and D). HIF1α levels associated with itraconazole monotherapy and in combination with cisplatin were 1.7 and 2.3 fold higher, respectively in LX-14 tumors, and 3.2 and 4.0 fold higher, respectively in LX-7 tumors, compared to vehicle-treatment. In contrast, tumor lysates from mice receiving cisplatin monotherapy demonstrated HIF1α expression levels equivalent to 0.8 and 0.9 fold that seen in vehicle treated LX-14 and LX-7 tumors, respectively.

To further interrogate the anti-angiogenic effects of itraconazole on lung cancer tumors *in vivo*, we directly analyzed tumor vascular perfusion by intravenous pulse administration of HOE dye immediately prior to euthanasia and tumor resection. This procedure allows for

assessment of functional vasculature based on fluorescent dye delivery to and concentration in perivascular nuclei. Analysis of perfused tumor sections by fluorescence microscopy demonstrated significant reduction of tumor microvessel density associated with itraconazole therapy in both LX-14 and LX-7 primary xenografts (Figure 5). Vehicle treated tumors demonstrated 14.9% and 21.9% mean tumor vascular area for LX-14 and LX-7 xenografts, respectively, whereas itraconazole mono-therapy resulted in reduction of mean tumor vascular area to 5.8% ($p<0.001$) and 9.7% ($p<0.001$) in LX-14 and LX-7 tumors, respectively. Addition of itraconazole to a cisplatin regimen resulted in a similarly significant decrease in tumor vasculature with LX-14 demonstrating a decrease in mean tumor vascular area from 11.2% to 6.1% ($p<0.001$) and LX-7 demonstrating a decrease from 20.8% to 10.3% ($p<0.001$) tumor vascular area.

DISCUSSION

Cancer-associated angiogenesis is a critical component of solid tumor establishment, growth, and spread, and remains a primary target of anti-cancer drug development (29). Anti-angiogenic therapies to date have primarily focused on two approaches: one, monoclonal antibodies or antibody derivatives that bind and sequester tumor-derived soluble endothelial growth factors or that inhibit ligand interaction with specific endothelial receptors; and two, small molecule tyrosine kinase inhibitors with specificity for endothelial receptors including VEGFR2 and FGFR3 (30). These strategies typically have a narrow focus, specifically targeting one of the most critical defined pathways of angiogenic stimulation. These novel drugs exemplify a broader ascendancy of rationally designed targeted therapeutic drug development as the predominant focus of therapeutic cancer research over the past 2 decades.

Narrowly targeted therapeutic strategies, the so-called “smart bombs” for cancer, are conceptually attractive in terms of selectively targeting tumor growth and survival pathways while limiting off-target toxicities. It is becoming clear that for complex biological processes such as cancer cell growth and angiogenic drive, focused inhibition of a critical node in a single signaling axis, even if the predominant signaling axis, invites emergence of resistance pathways. In lung cancer, most notably, targeting the driver mutation in EGFR mutant NSCLC can lead to dramatic initial responses in advanced disease, but is essentially never curative (31). Secondary mutations of EGFR itself (32), upregulation of alternative receptor tyrosine kinases such as c-MET (33; 34), constitutive activation of downstream pathways such as PI3K and Akt (35; 36), as well as a large scale shift in gene expression and morphology known as epithelial-mesenchymal transition (37; 38), have all been implicated as mechanisms of acquired resistance. These and similar observations have led to an ongoing debate about whether highly selective inhibitors or multi-targeted inhibitors will ultimately be more effective, and more durably effective, drugs.

Itraconazole as an anti-angiogenic agent appears to fall into the latter category, i.e. an inhibitor that coordinately affects multiple angiogenic stimulatory pathways. In this study, we evaluated the influence of itraconazole on multiple aspects of endothelial cell function that contribute to angiogenic potential. In assays of HUVEC proliferation, itraconazole consistently demonstrated potent anti-proliferative activity in cultures stimulated with a variety of growth factor conditions, including independent stimulation by VEGF and by bFGF alone. Although affecting multiple endothelial responses to multiple angiogenic stimuli, the proliferative inhibition of itraconazole appears reasonably cell type-specific, as much higher concentrations had essentially no effect on the proliferative capacity of five representative NSCLC cell lines, including cultures derived from two primary xenograft models. Probing of phosphorylation and activation status of receptor tyrosine kinases revealed that itraconazole has the capacity to inhibit activation of VEGFR2 and FGFR3, two

critical receptors primarily responsible for angiogenic response to these stimuli. Notably, alteration of VEGFR2 and FGFR3 phosphorylation state does not appear to be directly related to the previously noted effects of itraconazole on cholesterol trafficking and mTOR pathway inhibition (16). The mechanism(s) responsible for this targeted receptor inhibition has not been fully defined, and is the subject of ongoing analyses in our laboratories. These effects on multiple key drivers of angiogenesis may be important to the consistent inhibitory effects on multiple downstream angiogenic functions.

Beyond proliferation, endothelial cell migration, directional chemotaxis, and complex tube formation are all critical, and distinct, functional components of tumor-associated angiogenesis. Itraconazole potently inhibited each of these functional competencies as indicated by MTS, wound-healing, Boyden chamber, and tube formation assays. Extending these analyses *in vivo*, itraconazole demonstrated marked tumor growth inhibition in our primary xenograft models of squamous cell and adenocarcinoid NSCLC. When administered in combination with cytotoxic chemotherapy, itraconazole contributed to a durable cytostatic tumor growth response. These *in vivo* effects appeared to be consistent with a potent anti-angiogenic effect, associated with significant inhibition of angiogenic biomarkers, most notably intratumoral induction of the hypoxia responsive gene, HIF1α, and depletion of perfusion-competent tumor vasculature. Taken together, these *in vitro* and *in vivo* analyses support that itraconazole inhibits angiogenic potential across all models tested, and demonstrates intriguing efficacy in the first evaluation of this agent alone and in combination with cytotoxic chemotherapy in a pre-clinical primary cancer model.

Angiogenesis is an essential contributor to the growth and spread of solid tumors. Few anti-angiogenic agents have demonstrated improved outcomes in randomized phase III trials, including only one such agent in lung cancer patients studied to date. The benefits provided by bevacizumab in lung cancer represent an important proof of principle, yet these benefits are typically modest, improving survival by a few weeks in patients treated with first line chemotherapy. The lack of anti-angiogenic therapeutic options and limitations associated with bevacizumab therapy contribute to the need for development and evaluation of additional angiogenesis targeting agents, including agents with mechanisms of action distinct from the several monoclonal antibodies and tyrosine kinase inhibitors currently competing in this space. Itraconazole is an orally bioavailable, well-tolerated, widely available off-patent medication with a well-characterized safety profile in thousands of patients. The initial findings described here have important clinical implications for potential use of itraconazole as a novel anti-angiogenic agent and strongly support both further investigation of the molecular mechanisms of action of this drug in endothelial cells, and clinical investigation in patients with lung cancer and other solid tumors. Based on these several considerations, we have recently initiated a randomized phase II clinical trial randomizing patients with advanced recurrent NSCLC to standard chemotherapy with or without oral itraconazole.

Supplementary Material

Refer to Web version on PubMed Central for supplementary material.

Acknowledgments

Financial support: Flight Attendant Medical Research Institute, Burroughs Wellcome Fund, NIH P50 CA058184 (SPORE grant in lung cancer). We thank Hans Hammers, Craig Peacock, and members of the Rudin and Hann laboratories for discussion and advice regarding this work.

REFERENCES

1. Folkman J. Tumor Angiogenesis: Therapeutic Implications. N Engl J Med. 1971; 285:1182–1186. [PubMed: 4938153]
2. Niki T, Iba S, Tokunou M, Yamada T, Matsuno Y, Hirohashi S. Expression of vascular endothelial growth factors A, B, C, and D and their relationships to lymph node status in lung adenocarcinoma. Clin Cancer Res. 2000; 6:2431–2439. [PubMed: 10873096]
3. Han H, Silverman J, Santucci T, Macherey RS, dAmato TA, Tung MY, et al. Vascular Endothelial Growth Factor Expression in Stage I Non-Small Cell Lung Cancer Correlates With Neoangiogenesis and a Poor Prognosis. Ann Surg Oncol. 2001; 8:72–79. [PubMed: 11206229]
4. Bremnes RM, Camps C, Sirera R. Angiogenesis in non-small cell lung cancer: The prognostic impact of neoangiogenesis and the cytokines VEGF and bFGF in tumours and blood. Lung Cancer. 2006; 51:143–158. [PubMed: 16360975]
5. Asahara T, Bauters C, Zheng LP, Takeshita S, Bunting S, Ferrara N, et al. Synergistic effect of vascular endothelial growth factor and basic fibroblast growth factor on angiogenesis in vivo. Circulation. 1995; 92:365–371.
6. Seghezzi G, Patel S, Ren CJ, Gualandris A, Pintucci G, Robbins ES, et al. Fibroblast Growth Factor-2 (FGF-2) Induces Vascular Endothelial Growth Factor (VEGF) Expression in the Endothelial Cells of Forming Capillaries: An Autocrine Mechanism Contributing to Angiogenesis. J Cell Biol. 1998; 141:1659–1673. [PubMed: 9647657]
7. Cross MJ, Claesson-Welsh L. FGF and VEGF function in angiogenesis: signalling pathways, biological responses and therapeutic inhibition. Trends Pharmacol Sci. 2001; 22:201–207. [PubMed: 11282421]
8. American Cancer Society. Cancer Facts & Figures 2010. Atlanta: American Cancer Society; 2010.
9. Sandler A, Gray R, Perry MC, Brahmer J, Schiller JH, Dowlatiet A, et al. Paclitaxel–Carboplatin Alone or with Bevacizumab for Non–Small-Cell Lung Cancer. N Engl J Med. 2006; 355:2542–2550. [PubMed: 17167137]
10. Johnson DH, Fehrenbacher L, Novotny WF, Herbst RS, Nemunaitis JJ, Jablons DM, et al. Randomized Phase II Trial Comparing Bevacizumab Plus Carboplatin and Paclitaxel With Carboplatin and Paclitaxel Alone in Previously Untreated Locally Advanced or Metastatic Non-Small-Cell Lung Cancer. J Clin Oncol. 2004; 22:2184–2191. [PubMed: 15169807]
11. Ranpura V, Hapani S, Wu S. Treatment-Related Mortality With Bevacizumab in Cancer Patients. J Am Med Assoc. 2011; 305:487–494.
12. Fojo T, Grady C. How Much Is Life Worth: Cetuximab, Non-Small Cell Lung Cancer, and the $440 Billion Question. J Natl Cancer Inst. 2009; 101:1044–1048. [PubMed: 19564563]
13. Fojo T, Grady C. Response: Re: How Much Is Life Worth: Cetuximab, Non-Small Cell Lung Cancer, and the $440 Billion Question. J Natl Cancer Inst. 2010; 102:1207–1210. [PubMed: 20651322]
14. Reck M, von Pawel J, Zatloukal P, Ramlau R, Gorbounova V, Hirsh V, et al. Phase III Trial of Cisplatin Plus Gemcitabine With Either Placebo or Bevacizumab As First-Line Therapy for Nonsquamous Non–Small-Cell Lung Cancer: AVAiL. J Clin Oncol. 2009; 27:1227–1234. [PubMed: 19188680]
15. Chong CR, Xu J, Lu J, Bhat S, Sullivan DJ, Liu JO. Inhibition of angiogenesis by the antifungal drug itraconazole. ACS Chem Biol. 2007; 2:263–270. [PubMed: 17432820]
16. Xu J, Dang Y, Ren YR, Liu JO. Cholesterol trafficking is required for mTOR activation in endothelial cells. Proc Natl Acad Sci. U.S.A. 2010; 107:4764–4769. [PubMed: 20176935]
17. Kim J, Tang JY, Gong R, Kim J, Lee JJ, Clemons KV, et al. Itraconazole, a Commonly Used Antifungal that Inhibits Hedgehog Pathway Activity and Cancer Growth. Cancer Cell. 2010; 17:388–399. [PubMed: 20385363]
18. Lee J, Kotliarova S, Kotliarov Y, Li A, Su Q, Donin NM, et al. Tumor stem cells derived from glioblastomas cultured in bFGF and EGF more closely mirror the phenotype and genotype of primary tumors than do serum-cultured cell lines. Cancer Cell. 2006; 9:391–403. [PubMed: 16697959]

19. Embuscado EE, Laheru D. Immortalizing the complexity of cancer metastasis: Genetic features of lethal metastatic pancreatic cancer obtained from rapid autopsy. Cancer Biol Ther. 2005; 4:548–554. [PubMed: 15846069]
20. Morton CL, Houghton PJ. Establishment of human tumor xenografts in immunodeficient mice. Nat. Protocols. 2007; 2:247–250.
21. Daniel VC, Marchionni L, Hierman JS, Rhodes JT, Devereux WL, Rudin CM, et al. A Primary Xenograft Model of Small-Cell Lung Cancer Reveals Irreversible Changes in Gene Expression Imposed by Culture In vitro. Cancer Res. 2009; 69:3364–3373. [PubMed: 19351829]
22. O'Brien CA, Pollett A, Gallinger S, Dick JE. A human colon cancer cell capable of initiating tumour growth in immunodeficient mice. Nature. 2007; 445:106–110. [PubMed: 17122772]
23. Lefrançois D, Olschwang S, Delattre O, Muleris M, Dutrillaux AM, Thomas G, et al. Preservation of chromosome and DNA characteristics of human colorectal adenocarcinomas after passage in nude mice. Int J Cancer. 1989; 44:871–878. [PubMed: 2573580]
24. Rijken PFJW, Bernsen HJJA, van der Kogel AJ. Application of an Image Analysis System to the Quantitation of Tumor Perfusion and Vascularity in Human Glioma Xenografts. Microvasc Res. 1995; 50:141–153. [PubMed: 8538495]
25. Franco M, Man S, Chen L, Emmenegger U, Shaked Y, Cheung AM, et al. Targeted Anti–Vascular Endothelial Growth Factor Receptor-2 Therapy Leads to Short-term and Long-term Impairment of Vascular Function and Increase in Tumor Hypoxia. Cancer Res. 2006; 66:3639–3648. [PubMed: 16585189]
26. Zeng H, Dvorak HF, Mukhopadhyay D. Vascular permeability factor (VPF)/vascular endothelial growth factor (VEGF) peceptor-1 down-modulates VPF/VEGF receptor-2-mediated endothelial cell proliferation, but not migration, through phosphatidylinositol 3-kinase-dependent pathways. J Biol Chem. 2001; 276:26969–26979. [PubMed: 11350975]
27. Lamalice L, Le Boeuf F, Huot J. Endothelial Cell Migration During Angiogenesis. Circ Res. 2007; 100(6):782–794. [PubMed: 17395884]
28. Montesano R. In vitro rapid organization of endothelial cells into capillary-like networks is promoted by collagen matrices. J Cell Biol. 1983; 97:1648–1652. [PubMed: 6630296]
29. Hicklin DJ, Ellis LM. Role of the Vascular Endothelial Growth Factor Pathway in Tumor Growth and Angiogenesis. J Clin Oncol. 2005; 23:1011–1027. [PubMed: 15585754]
30. Herbst RS. Therapeutic options to target angiogenesis in human malignancies. Expert Opin Emerging Drugs. 2011; 11:635–650.
31. Jänne PA, Gray N, Settleman J. Factors underlying sensitivity of cancers to small-molecule kinase inhibitors. Nat Rev Drug Discov. 2009; 8:709–723. [PubMed: 19629074]
32. Kobayashi S, Boggon TJ, Dayaram T, Jänne PA, Kocher O, Meyerson M, et al. EGFR Mutation and Resistance of Non–Small-Cell Lung Cancer to Gefitinib. N Engl J Med. 2005; 352:786–792. [PubMed: 15728811]
33. Engelman JA, Zejnullahu K, Mitsudomi T, Song Y, Hyland C, Park JO, et al. MET Amplification Leads to Gefitinib Resistance in Lung Cancer by Activating ERBB3 Signaling. Science. 2007; 316:1039–1043. [PubMed: 17463250]
34. Zucali PA, Ruiz MG, Giovannetti E, Destro A, Varella-Garcia M, Floor K, et al. Role of cMET expression in non-small-cell lung cancer patients treated with EGFR tyrosine kinase inhibitors. Ann Oncol. 2008; 19:1605–1612. [PubMed: 18467317]
35. She Q-B, Solit D, Basso A, Moasser MM. Resistance to Gefitinib in PTEN-Null HER-Overexpressing Tumor Cells Can Be Overcome through Restoration of PTEN Function or Pharmacologic Modulation of Constitutive Phosphatidylinositol 3′-Kinase/Akt Pathway Signaling. Clin Cancer Res. 2003; 9:4340–4346. [PubMed: 14555504]
36. Janmaat ML, Kruyt FAE, Rodriguez JA, Giaccone G. Response to Epidermal Growth Factor Receptor Inhibitors in Non-Small Cell Lung Cancer Cells. Clin Cancer Res. 2003; 9:2316–2326. [PubMed: 12796401]
37. Thomson S, Buck E, Petti F, Griffin G, Brown E, Ramnarine N, et al. Epithelial to Mesenchymal Transition Is a Determinant of Sensitivity of Non–Small-Cell Lung Carcinoma Cell Lines and Xenografts to Epidermal Growth Factor Receptor Inhibition. Cancer Res. 2005; 65:9455–9462. [PubMed: 16230409]

38. Buck E, Eyzaguirre A, Barr S, Thompson S, Sennello R, Young D, et al. Loss of homotypic cell adhesion by epithelial-mesenchymal transition or mutation limits sensitivity to epidermal growth factor receptor inhibition. Mol Cancer Ther. 2007; 6:532–541. [PubMed: 17308052]

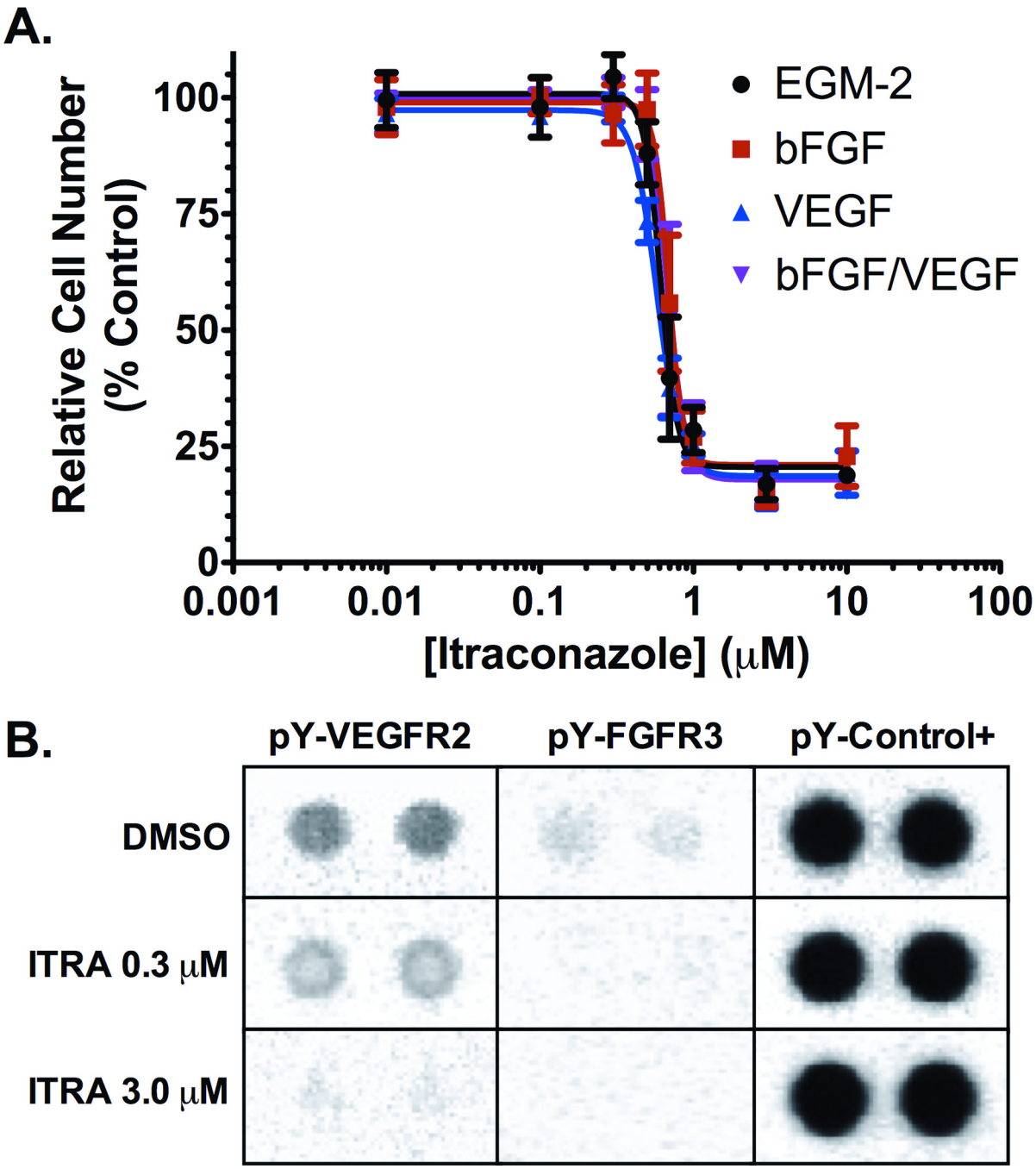

Figure 1. Inhibition of proliferation and receptor tyrosine kinase phosphorylation in stimulated HUVEC cultures

(A) Itraconazole inhibits HUVEC proliferation in a dose dependent manner in cultures stimulated by supplementation with EGM-2 (black), 12 ng/ml bFGF (red), 10 ng/ml VEGF (blue), and 12 ng/ml bFGF with 10 ng/ml VEGF (purple). Mean relative cell number was evaluated by MTS assay and are reported as mean percent of vehicle treated cell proliferation ± SD. **(B)** Cell lysates from EGM-2 stimulated HUVEC treated with 0.3 μM or 3.0 μM itraconazole, or with vehicle control for 24 h were hybridized to an RTK array and probed with anti-phospho-tyrosine-HRP antibody followed by chemiluminescent detection.

Each RTK is spotted in duplicate with signal normalized to phospho-tyrosine internal controls.

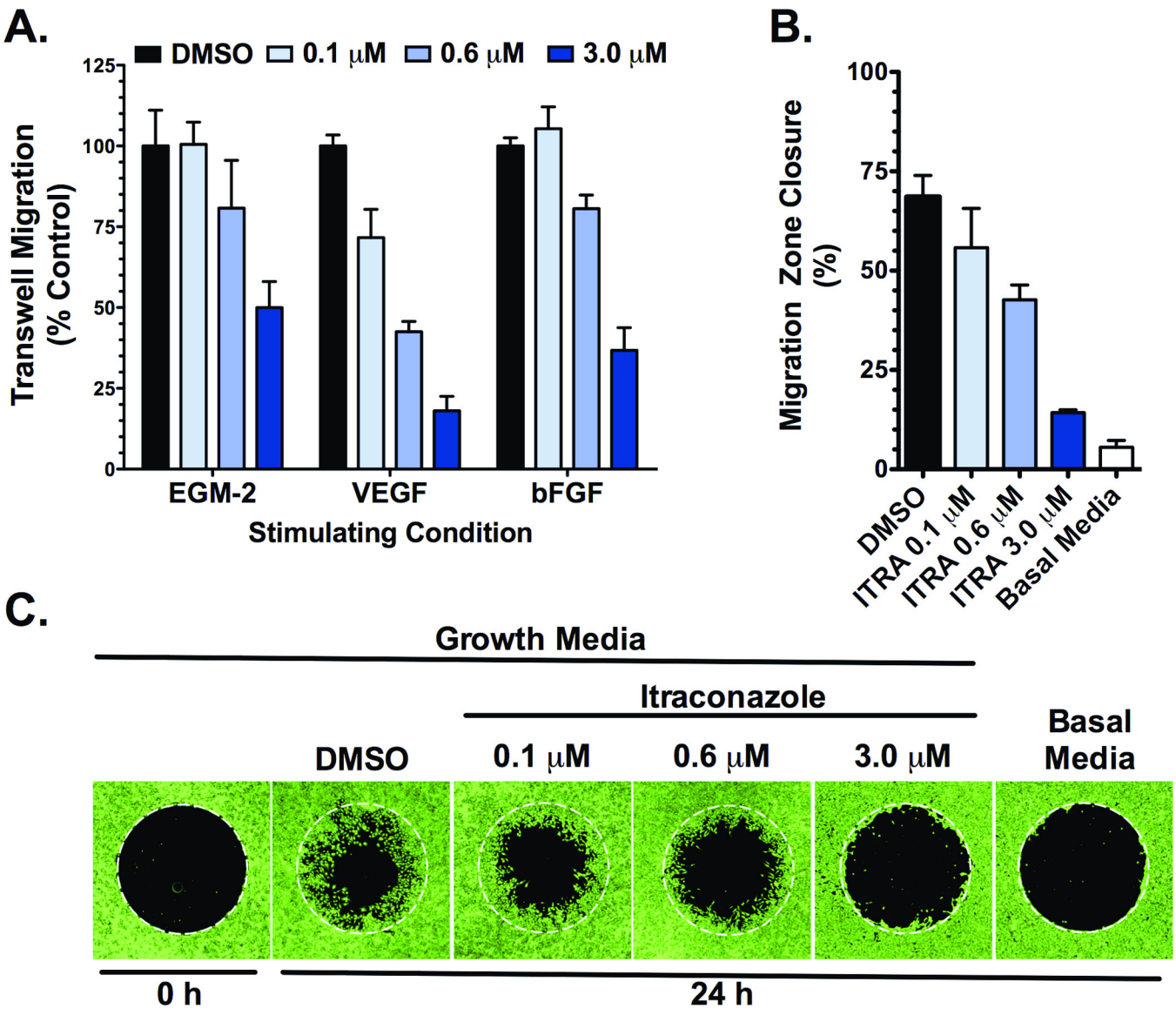

Figure 2. Itraconazole inhibits migration of stimulated HUVEC

(A) HUVEC demonstrate decreased migratory potential across EGM-2, VEGF, and bFGF chemotactic gradients in the presence of increasing concentrations of itraconazole in a transwell assay. Corrected means ± SD of total DNA content from migratory cells are reported as percent of vehicle control for each stimulating condition. **(B & C)** Itraconazole inhibits EGM-2 stimulated HUVEC migration in a modified wound-healing assay. Following attachment, cells were treated with EGM-2 media containing DMSO vehicle control or 0.1 μM, 0.6 μM, or 3.0 μM itraconazole and permitted to migrate over 24 h into the previously restricted region. Basal media serves as control for unstimulated migration. **(B)** Migration was quantified as the percent decrease in mean migration zone area ± SD. **(C)** Representative fluorescence images from the modified wound-healing assay with cells stained by calcein-AM, after a 24 h migration period.

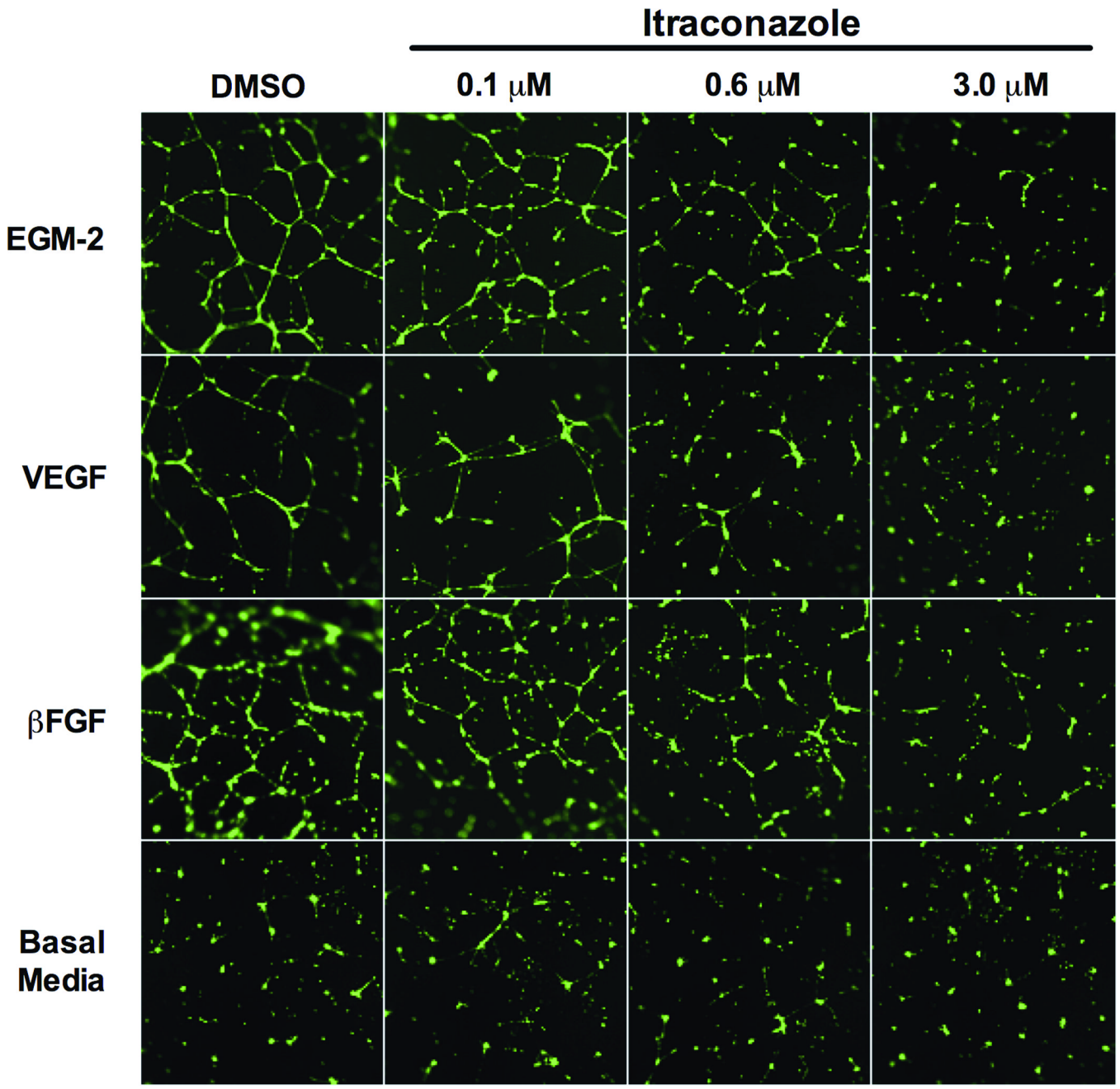

Figure 3. Itraconazole inhibits EGM-2, VEGF, and bFGF stimulated HUVEC tube formation

HUVEC stimulated with EGM-2, 10 ng/ml VEGF, or 12 ng/ml bFGF were allowed to spontaneously form tube networks after treatment with vehicle control, 0.1 μM, 0.6 μM, or 3.0 μM itraconazole. Unstimulated (basal media) HUVEC serve as negative control. Resulting networks were visualized with calcein-AM.

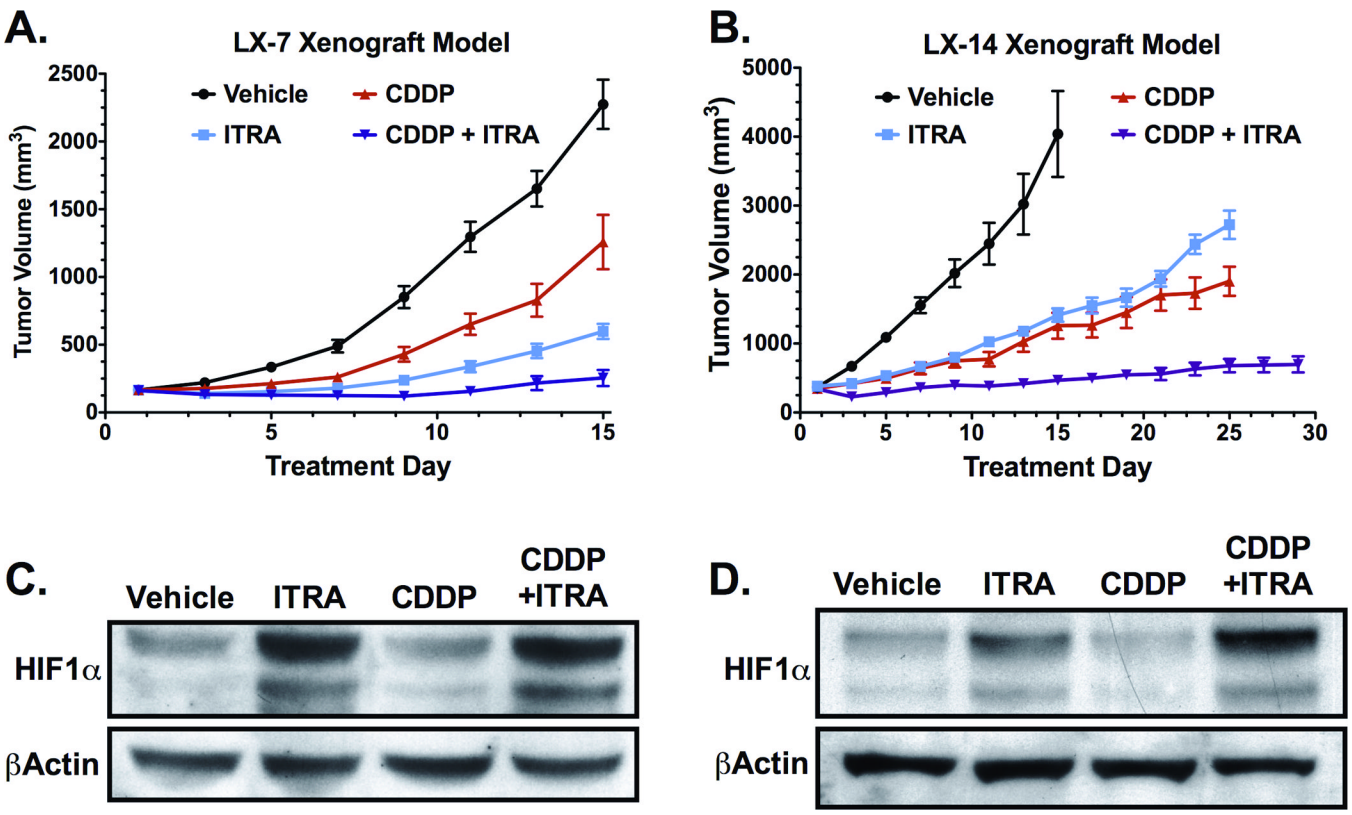

Figure 4. Itraconazole inhibits growth of NSCLC primary xenografts, with itraconazole treated tumors demonstrating increased levels of HIF1α

(A) Mice bearing established LX-7 tumors were treated with vehicle (n=9), oral itraconazole 100 mg/kg bid (ITRA, n=9), cisplatin 4 mg/kg q7d i.p. (CDDP, n=9), or combination itraconazole and cisplatin (ITRA+CDDP, n=8). Mean tumor volume and SEM are reported for each treatment group. **(B)** Mice bearing established LX-14 tumors were treated with vehicle (n=6), oral itraconazole 100 mg/kg bid (ITRA, n=7), cisplatin 4 mg/kg q7d i.p. (CDDP, n=6), or combination itraconazole and cisplatin (ITRA+CDDP, n=7). Mean tumor volume and SEM are reported for each treatment group. **(C)** Tumor lysates from LX-7 xenografts were generated from mice treated for 14-days with vehicle (n=4), oral itraconazole (ITRA, n=4), i.p. cisplatin (CDDP, n=4), or combination of itraconazole and cisplatin (ITRA+CDDP, n=4). Pooled lysates were probed for HIF1α. **(D)** HIF1α immunoblot on pooled tumor lysates from LX-14 xenografts treated for 14-days with vehicle (n=4), oral itraconazole (ITRA, n=4), i.p. cisplatin (CDDP, n=4), or combination of itraconazole and cisplatin (ITRA+CDDP, n=3).

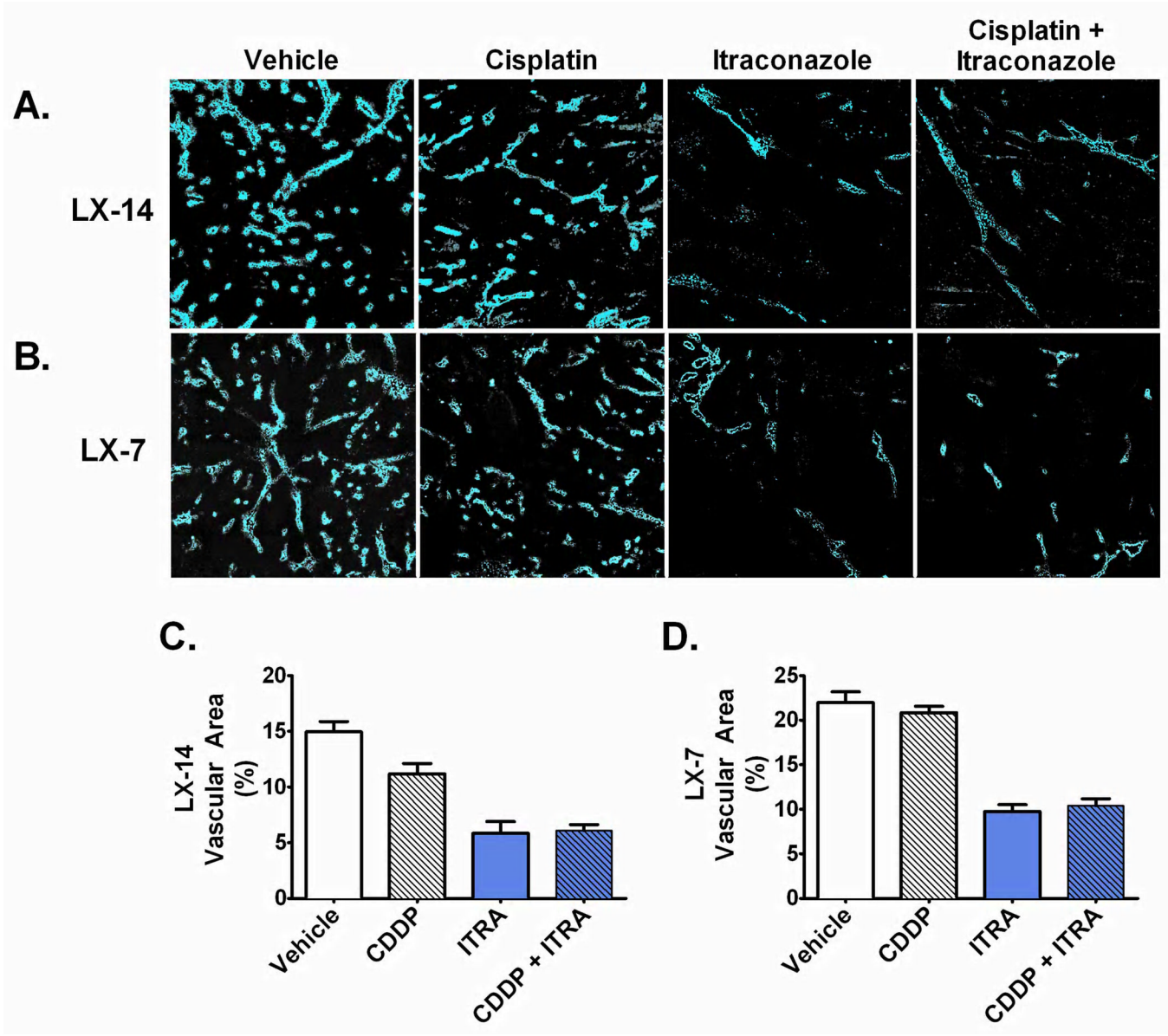

Figure 5. NSCLC tumors demonstrate decreased microvessel density and tumor vascular area following itraconazole treatment

HOE signal from **(A)** perfused LX-14 tumor and **(B)** perfused LX-7 sections demonstrate marked decrease in perfusion-competent microvessel density in itraconazole treated tumors. **(C & D)** Mean ± SEM HOE-positive tumor vascular area in **(C)** LX-14 tumors treated with vehicle (n=5), itraconazole (ITRA, n=6), cisplatin (CDDP, n=5), or combination itraconazole and cisplatin (ITRA+CDDP, n=7); **(D)** LX-7 tumors treated with vehicle (n=5), itraconazole (ITRA, n=5), cisplatin (CDDP, n=5), or combination itraconazole and cisplatin (ITRA+CDDP, n=5).